Two Birds One Stone: Blind Beamforming for Integrated Communications and Localization

Wenhai Lai, Kaiming Shen, and Zhi-Quan Luo
School of Science and Engineering, The Chinese University of Hong Kong (Shenzhen), China
E-mail: wenhailai@link.cuhk.edu.cn, shenkaiming@cuhk.edu.cn, luozq@cuhk.edu.cn

***Abstract*—This paper considers a typical application case of the integrated sensing and communications (ISAC) in which the receiver wishes to not only enhance its channel capacity but also localize the transmitter in aid of metasurfaces (MTSs). In view of practical situations, we assume that the MTSs consist of low-resolution (e.g., 1-bit) phase shifters and that the channel state information (CSI) is completely unknown. The key step in the proposed method is to retrieve the phase difference information from the received signal strength (RSS) through a novel technique called *blind beamforming*. We then utilize the phase difference information to align the reflected channels and thereby enhance signal-to-noise ratio (SNR), and also recover the position of the target with the MTSs treated as anchors. According to our field tests carried out at 2.6 GHz frequency band, the proposed method gives much more precise localization than the benchmarks, aside from increasing the SNR by up to around 10 dB.**

I. Introduction

Metasurface (MTS) is a planar array of meta-atoms. Each meta-atom is programmable in the sense that it can reconfigure the phase shift of the incident electromagnetic signal. There are two popular applications: (i) use MTS to focus the reflecting beam onto the receiver to increase its signal-to-noise ratio (SNR) and thereby improve the quality of communications; (ii) use multiple MTSs as anchors to facilitate localization. The central problem here is to optimize the phase shifts of MTSs, which has been dealt with separately for communications and localization in the literature. In contrast, this work proposes a unified blind beamforming method to accomplish the two purposes simultaneously.

Unlike conventional wireless communication technologies that focus on the transmitter/receiver-side design, MTS aims to improve the propagation environment by manipulating reflected paths. When the channel state information (CSI) is available, a variety of standard tools are applicable for the optimization of phase shifts of MTS, including the semidefinite relaxation (SDR) [1], [2], the minorization-maximization (MM) [3], and the fractional programming (FP) [4], [5]. The aforementioned CSI-based methods all rely on precise real-time channel acquisition—which is difficult to guarantee in practice for the following reasons: (i) each reflected channel alone is much weaker than the direct channel plus the background noise, so the estimation error can be quite large; (ii) MTS typically comprises hundreds of meta-atoms, so channel estimation is computationally formidable; (iii) additional channel estimation for MTS requires modifying the existing network protocol. As such, this work considers the phase shift optimization of MTS in the absence of CSI. Our approach is most closely related to the so-called RFocus algorithm in [6], which extracts features of the wireless environment from the received signal strength (RSS) and optimizes the phase shifts accordingly. The proposed method called the *blind phase shift optimizer (BPSO)* differs from the RFocus algorithm in two places. First, our method works for a wider range of MTS models. Second, more importantly, our method accounts for the localization task aside from the communication task.

While the conventional use of MTS is focused on wireless communications, there has been an emerging research interest in the MTS-assisted localization over the past few years. The idea of treating MTS as "anchor" is proposed for both indoor and outdoor localization cases [7], [8]. The authors of [9] devise a so-called MetaSight system to localize a radio frequency identification (RFID) object by using a pair of MTSs. Its main idea is to acquire the phase information for all the reflected channels related to the MTSs and subsequently deduce the angle of arrival (AoA) from each MTS to the target. Each MTS gives an angle measure, so we can decide the target position by intersecting the two angle measures. Clearly, the core of the above technology lies in the phase acquisition for reflected channels. In contrast, [10] also employs two MTSs but does not require estimating phases. The proposed method in [10] performs beam scanning exhaustively to determine the angles. It is worth noting that the beam scanning method has also been considered for the MTS-assisted communications [11], [12]. Our method BPSO is more related to the phase-based method in [9]. Our field tests show that the proposed method outperforms the beam scanning method significantly in both communications and localization tasks.

II. System Model

Consider a double-MTS system as shown in Fig. 1. Each MTS acts as an anchor to determine one direction of the target, so a pair of MTSs suffice to determine the 2D location. Assume that each MTS consists of N meta-atoms arranged as an $N_z \times N_y$ array, where $N = N_z N_y$. The (u, v)th meta-atom refers to the meta-atom on the uth row and the vth column, for $u = 1, 2, \ldots, N_z$ and $v = 1, 2, \ldots, N_y$. The positions of the two MTSs are precisely known *a priori*. Denote by $\theta_{\ell,u,v}$

This work was supported in part by the NSFC under Grant 12426306, in part by Guangdong Basic and Applied Basic Research under Grant 2023B0303000001, and in part by Shenzhen Steady Funding Program. *(Corresponding author: Kaiming Shen.)*

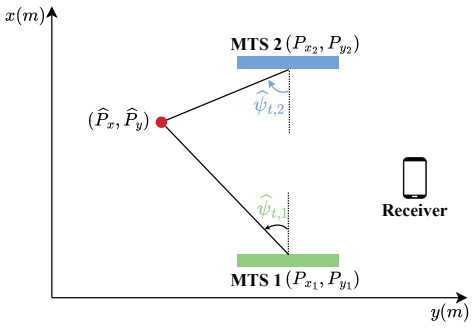

Fig. 1. Localizing the transmitter by taking the two MTSs as anchors.

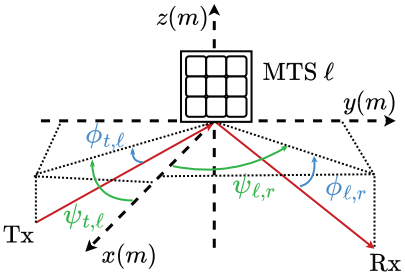

Fig. 2. Azimuth and elevation angles from each MTS to transmitter/receiver.

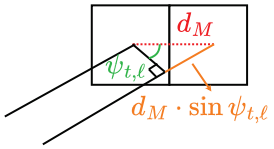

Fig. 3. Path distance difference between two horizontally adjacent meta-atoms.

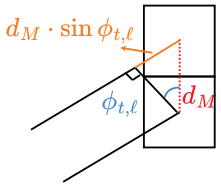

Fig. 4. Path distance difference between two vertically adjacent meta-atoms.

the phase shift of the (u,v)th meta-atom of MTS $\ell \in \{1,2\}$. Let $\boldsymbol{\theta}_\ell = \{\theta_{\ell,u,v}, \forall u,v\}$ be the set of phase shift variables for MTS ℓ. These phase shifts are subject to practical finite-resolution constraints, e.g., for the $(\log_2 K)$-bit phase shifter case, the choice of each $\theta_{\ell,u,v}$ is limited to a discrete set $\Phi_K = \{0, \omega, 2\omega, \ldots, (K-1)\omega\}$, where $\omega = \frac{2\pi}{K}$.

Denote by $h_{t,r} \in \mathbb{C}$ the direct channel from transmitter to receiver, $h_{t,\ell,u,v} \in \mathbb{C}$ the channel from transmitter to the (u,v)th meta-atom of MTS ℓ, $h_{\ell,r,u,v} \in \mathbb{C}$ the channel from the (u,v)th meta-atom of MTS ℓ to receiver. Each of the above channels is modeled as

$$h = \sqrt{\gamma}\left(\sqrt{\frac{\delta}{1+\delta}}\overline{h} + \sqrt{\frac{1}{1+\delta}}\widetilde{h}\right), \tag{1}$$

where $0 < \gamma < 1$ is the attenuation factor, $\delta > 0$ is the Rician factor, $\overline{h} \in \mathbb{C}$ is the line-of-sight (LOS) component satisfying $|\overline{h}| = 1$, and the fading component $\widetilde{h}$ is a random variable drawn from the complex Gaussian distribution $\mathcal{CN}(0,1)$. Note that the parameters $(\gamma, \delta, \overline{h})$ can vary from channel to channel, while the random variables $\widetilde{h}$ are i.i.d. across the channels. Thus, the (u,v)th meta-atom of MTS ℓ induces the following reflected channel from transmitter to receiver:

$$h_{\ell,u,v} = h_{t,\ell,u,v} \times h_{\ell,r,u,v}, \ \ell \in \{1,2\}. \tag{2}$$

Furthermore, the LOS channels can be computed explicitly. Denote by $(\psi_{t,\ell}, \phi_{t,\ell}, \psi_{\ell,r}, \phi_{\ell,r})$ the azimuth and elevation angles associated with MTS ℓ as illustrated in Fig. 2, denote by λ_c the carrier frequency, and denote by d_M the spacing between two adjacent meta-atoms. Fig. 3 (resp. Fig. 4) shows the path length difference between two adjacent meta-atoms on the same row (resp. column) for the incident signal. With the top-left meta-atom index as $(1,1)$, we can obtain from geometry the phases of the LOS components as

$$\begin{aligned}
\angle\overline{h}_{t,\ell,u,v} &= \xi d_M\big(v\sin(\psi_{t,\ell})\cos(\phi_{t,\ell}) - u\sin(\phi_{t,\ell})\big) + \xi d_{t,\ell},\\
\angle\overline{h}_{\ell,r,u,v} &= \xi d_M\big(u\sin(\phi_{\ell,r}) - v\sin(\psi_{\ell,r})\cos(\phi_{\ell,r})\big) - \xi d_{\ell,r},\\
\angle\overline{h}_{t,r} &= \xi d_{t,r},
\end{aligned} \tag{3}$$

where $\xi = -\frac{2\pi}{\lambda_c}$ and $\{d_{t,\ell}, d_{\ell,r}, d_{t,r}\}$ are the distances as indicated by their subscripts.

For wireless communication, we aim to maximize the expected overall channel power by coordinating the phase shifts of MTSs:

$$\text{SNR} = \mathbb{E}\left[\left|h_{t,r} + \sum_{\ell=1}^{2}\sum_{u=1}^{N_z}\sum_{v=1}^{N_y}\left(h_{\ell,u,v}e^{j\theta_{\ell,u,v}}\right)\right|^2\right], \tag{4}$$

where the expectation is taken over the fading components. In the meanwhile, we wish to localize the transmitter based on the RSS measure as the receiver, namely *active sensing*, by using the two MTSs as anchors. Denote by $(\widehat{P}_x, \widehat{P}_y) \in \mathbb{R}^2$ the estimated position coordinates of the transmitter and denote by (P_x, P_y) the ground truth. Without any CSI, we can only obtain $(\widehat{P}_x, \widehat{P}_y)$ from the RSS measure at the receiver side. We seek to minimize the mean squared estimation error:

$$\text{MSE} = \mathbb{E}\big[(P_x - \widehat{P}_x)^2 + (P_y - \widehat{P}_y)^2\big], \tag{5}$$

where the expectation is taken over the fading components.

III. Communication Enhancement

We start with the communication task alone. This section extends the main result in [13] for the double-MTS system: how to maximize the expected overall channel power in (4) without CSI. First, we generate each $\theta_{\ell,u,v}$ randomly and independently, and then measure the corresponding RSS, written as S, at the receiver; each S corresponds to a random sample. We perform a total of T random samples. For the tth random sample, let $\boldsymbol{\theta}_1^t = \{\theta_{1,u,v}^t\}$ be the set of phase shifts of MTS 1, let $\boldsymbol{\theta}_2^t = \{\theta_{2,u,v}^t\}$ be the set of phase shifts of MTS 2, and let S^t be the RSS. The T random samples are then grouped as follows. Let $\mathcal{Q}_{\ell,u,v,k}$ be the set of indices of those random samples whose phase shift for the (u,v)th meta-atom of MTS ℓ equals $k\omega$, i.e., $\mathcal{Q}_{\ell,u,v,k} = \{t \mid \theta_{\ell,u,v}^t = k\omega\}$, for $k = 1, \ldots, K$. We then compute the conditional sample mean

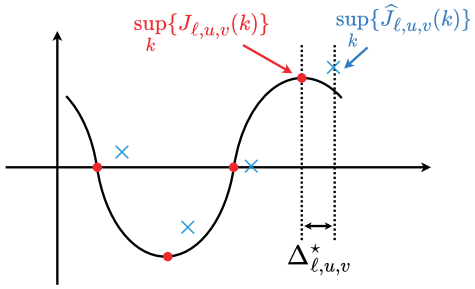

Fig. 5. The CSM method can be interpreted as finding the optimal $\Delta_{\ell,u,v}$ to match $\sup_k\{J_{\ell,u,v}(k)\}$ with $\sup_k\{\widehat{J}_{\ell,u,v}(k)\}$.

of RSS within each $\mathcal{Q}_{\ell,u,v,k}$ as

$$\widehat{\mathbb{E}}\left[S \mid \theta_{\ell,u,v} = k\omega\right] = \frac{1}{|\mathcal{Q}_{\ell,u,v,k}|}\sum_{t\in\mathcal{Q}_{\ell,u,v,k}} S^t. \tag{6}$$

Finally, we choose each phase shift to maximize the conditional sample mean of RSS:

$$\theta^\star_{\ell,u,v} = \arg\max_{\varphi\in\Phi_K} \widehat{\mathbb{E}}\left[S \mid \theta_{\ell,u,v} = \varphi\right]. \tag{7}$$

As such, the above algorithm is referred to as the conditional sample mean (CSM) algorithm, which extends the result in [13]. Following the steps in [13], we can show that $\mathrm{SNR} \propto N^2$ for T sufficiently large (in a polynomial order).

IV. Connection to Phase Difference Retrieval

As a key insight provided in [13], the CSM algorithm can boost the expected overall channel power because it can align each reflected channel $\overline{h}_{\ell,u,v} = \overline{h}_{t,\ell,u,v} \times \overline{h}_{\ell,r,u,v}$ with the direct channel $\overline{h}_{t,r}$ as much as possible in the absence of CSI. Actually, we can take advantage of this alignment effect to perform the phase difference retrieval. To be more specific, we can recover the phase difference between $\overline{h}_{\ell,u,v}$ and $\overline{h}_{t,r}$ from the output of the CSM algorithm.

First, with all the phase shifts generated randomly and independently, we define the following function in $k = 1, \ldots, K$:

$$\begin{aligned} J_{\ell,u,v}(k) &= \mathbb{E}\left[S \mid \theta_{\ell,u,v} = k\omega\right] - \mathbb{E}\left[S\right] \\ &= PA_{\ell,u,v}\cos(k\omega - \Delta_{\ell,u,v}), \end{aligned} \tag{8}$$

where

$$\Delta_{\ell,u,v} = \angle\overline{h}_{t,r} - \angle\overline{h}_{\ell,u,v} \tag{9}$$

is the phase difference, $A_{\ell,u,v}$ is a constant, and P is the transmit power. Although $J_{\ell,u,v}(k)$ depends on the CSI, we can empirically evaluate it based on the RSS measures:

$$\begin{aligned} \widehat{J}_{\ell,u,v}(k) &= \widehat{\mathbb{E}}\left[S \mid \theta_{\ell,u,v} = k\omega\right] - \widehat{\mathbb{E}}\left[S\right] \\ &= \frac{1}{|\mathcal{Q}_{\ell,u,v,k}|}\sum_{t\in\mathcal{Q}_{\ell,u,v,k}} S^t - \frac{1}{T}\sum_{t=1}^{T} S^t. \end{aligned} \tag{10}$$

Now we aim to minimize the distortion between $J_{\ell,u,v}(k)$ and $\widehat{J}_{\ell,u,v}(k)$ by tuning the phase difference $\Delta_{\ell,u,v}$ in (8). In particular, if we choose a square-of-max metric:

$$\beta_{\ell,u,v}(\Delta_{\ell,u,v}) = \left|\sup_k\{J_{\ell,u,v}(k)\} - \sup_k\{\widehat{J}_{\ell,u,v}(k)\}\right|^2, \tag{11}$$

then the distortion minimization problem is

$$\underset{\{\Delta_{\ell,u,v}\}}{\text{minimize}} \quad \sum_{\ell,u,v}\beta_{\ell,u,v}(\Delta_{\ell,u,v}) \tag{12a}$$

$$\text{subject to} \quad \Delta_{\ell,u,v} \in (0, 2\pi],\ \forall(\ell,u,v). \tag{12b}$$

The above problem can be optimally solved in closed form as $\Delta^\star_{\ell,u,v} = k^\star_{\ell,u,v}\omega$ with $k^\star_{\ell,u,v} = \arg\max_k \widehat{J}_{\ell,u,v}(k)$, as illustrated in Fig. 5. This solution can be thought of as an estimate of the unknown phase difference $\Delta_{\ell,u,v}$ in (9), which can be further recognized as the solution by the CSM method in [13]. Indeed, we hit two birds with one stone: the random sampling in the CSM algorithm not only yields the phase shift solution $\{\theta_{\ell,u,v}\}$ that guarantees $\mathrm{SNR} \propto N^2$, but also recovers the phase difference $\Delta_{\ell,u,v}$ that plays a central role in the MTS-based localization as discussed in the next section.

V. Localization Based on Phase Difference

After obtaining the phase difference information $\{\Delta^\star_{\ell,u,v}\}$ as shown in the previous section, we are ready to localize the target by using the geometric relationships in (3). First, by substituting $\angle\overline{h}_{t,r}$, $\angle\overline{h}_{t,\ell,u,v}$, and $\angle\overline{h}_{\ell,r,u,v}$ into (9), we rewrite $\Delta_{\ell,u,v}$ as in (13). Equipped with (13), we show that the phase difference for any two *vertically adjacent* meta-atoms (u,v) and $(u+1,v)$ can be determined as

$$\Delta_{\ell,u+1,v} - \Delta_{\ell,u,v} = \xi d_M\big(\sin(\phi_{\ell,r}) - \sin(\phi_{t,\ell})\big). \tag{14}$$

Recall that $\phi_{\ell,r}$ only depends on the position of the MTS anchor, which is available since the position of MTS is already known. Recall also that we can recover $\Delta_{\ell,u,v}$ as $\Delta^\star_{\ell,u,v}$ by performing the CSM method. Thus, through (14), we can recover $\phi_{t,\ell}$ as

$$\phi^\star_{t,\ell,u,v} = \arcsin\left(\sin(\phi_{\ell,r}) - \frac{\Delta^\star_{\ell,u+1,v} - \Delta^\star_{\ell,u,v}}{\xi d_M}\right). \tag{15}$$

There are $(N_z-1)N_y$ pairs of vertically adjacent meta-atoms on each MTS in total. We compute $\phi^\star_{t,\ell,u,v}$ for each pair and then average out to get the ultimate estimate $\widehat{\phi}_{t,\ell}$.

The above procedure can be extended for the horizontally adjacent meta-atoms. Similarly, we show that any two *horizontally adjacent* meta-atoms (u,v) and $(u,v+1)$ have their phase difference:

$$\begin{aligned} &\Delta_{\ell,u,v+1} - \Delta_{\ell,u,v} = \\ &\quad \xi d_M\big(\sin(\psi_{t,\ell})\cos(\phi_{t,\ell}) - \sin(\psi_{\ell,r})\cos(\phi_{\ell,r})\big). \end{aligned} \tag{16}$$

$$\Delta_{\ell,u,v} = \xi d_{t,r} - \xi d_M\cdot v\big(\sin(\psi_{\ell,r})\cos(\phi_{\ell,r}) - \sin(\psi_{t,\ell})\cos(\phi_{t,\ell})\big) - \xi d_M\cdot u\big(\sin(\phi_{t,\ell}) - \sin(\phi_{\ell,r})\big) + \xi(d_{t,\ell} - d_{\ell,r}). \tag{13}$$

Algorithm 1 Proposed BPSO method

input: T random samples of $(\boldsymbol{\theta}_1^t, \boldsymbol{\theta}_2^t)$
for $t = 1, 2, \ldots, T$ **do**
    set the MTS phase shifts as $(\boldsymbol{\theta}_1^t, \boldsymbol{\theta}_2^t)$
    measure the corresponding RSS S^t
end for
compute $\widehat{\mathbb{E}}\left[S \mid \theta_{\ell,u,v} = k\omega\right]$ according to (6)
decide $\theta_{\ell,u,v}$ and recover $\Delta^{\star}_{\ell,u,v}$ according to (7)
recover elevation angle $\widehat{\phi}_{t,\ell}$ and azimuth angle $\widehat{\psi}_{t,\ell}$
find the location $(\widehat{P}_x, \widehat{P}_y)$ by solving (18)
output: optimized $\{\theta_{\ell,u,v}\}$ and the coordinates $(\widehat{P}_x, \widehat{P}_y)$

We then estimate $\psi_{t,\ell}$ based on (16) as

$$\psi^{\star}_{t,\ell,u,v} = \arcsin\left(\frac{\Delta^{\star}_{\ell,u,v+1} - \Delta^{\star}_{\ell,u,v}}{\xi d_M \cos(\widehat{\phi}_{t,\ell})} + \frac{\sin(\psi_{\ell,r})\cos(\phi_{\ell,r})}{\cos(\widehat{\phi}_{t,\ell})}\right). \quad (17)$$

Subsequently, we average out the above estimation across all $(N_y - 1)N_z$ possible pairs of horizontally adjacent meta-atoms on each MTS to arrive at the ultimate estimate $\widehat{\psi}_{t,\ell}$.

After recovering the elevation angle $\phi_{t,\ell}$ and the azimuth angle $\psi_{t,\ell}$ from MTS ℓ to the target, we can draw a ray connecting MTS ℓ and the target. Since there are two MTSs at distinct positions, we can locate the target at the intersection of the two rays, as shown in Fig. 1. Specifically, denoting by (P_{x_1}, P_{y_1}) and (P_{x_2}, P_{y_2}) the locations of the two MTSs (in terms of their center points), we can obtain the estimate $(\widehat{P}_x, \widehat{P}_y)$ by solving the following system of linear equations:

$$y - P_{y_1} = -\tan(\widehat{\psi}_{t,1})(x - P_{x_1}), \quad (18a)$$
$$y - P_{y_2} = \tan(\widehat{\psi}_{t,2})(x - P_{x_2}). \quad (18b)$$

Algorithm 1 summarizes all the steps of our proposed BPSO method for enhancing communication and localization jointly.

VI. Field Tests

As shown in Fig. 6, we implement a double-MTS system in an indoor classroom. As shown in Fig. 7, the MTS prototype comprises $21 \times 14 = 294$ meta-atoms separated by 6 cm. Each meta-atom provides 2 phase shift options $\{0, \pi\}$. The operating frequency of the MTS prototype is 2.6 GHz. The positions of the transmitter and the receiver are fixed at coordinates $(0, 0.53, 0.1)$ and $(4.51, -0.48, 0.1)$, respectively. The two MTSs are placed at $(1.24, -1.25, 1.56)$ for MTS 1 and $(1.24, 1.35, 1.56)$ for MTS 2. The transmitter is equipped with an omnidirectional antenna. To compare with traditional localization algorithms based on the antenna array, we deploy four omnidirectional antennas at the receiver, but for communication performance, we only consider the SNR of a single antenna. We send the signal at a carrier frequency of 2.6 GHz, with a bandwidth of 125 KHz.

For communication performance, we compare the proposed BPSO with several existing benchmarks:

- *Zero Phase Shifts (ZPS):* Fix phase shifts to zero.
- *Beam Scanning [11], [12]:* Try out T random samples and then choose the best.
- *DFT:* First estimate the channel by the discrete Fourier transform (DFT)-based method in [14] and then optimize the phase shifts of two MTSs.
- *ALRA:* First estimate the channel by the approximate low-rank-approaching (ALRA) method in [15] and then optimize the phase shifts of two MTSs.

We compare the performance of the BPSO with the above methods in terms of the SNR boost at the receiver compared to the system without MTS. Moreover, we compare the localization accuracy of the proposed BPSO with the following methods:

- *MUSIC:* Removing the two MTSs from the system, the receiver executes the localization algorithm based on the MUSIC algorithm.
- *MUSIC-ZPS:* The receiver performs the same localization algorithm in *MUSIC*, but we deploy the two MTSs in the system with zero phase shifts.
- *DFT:* Use the DFT method in [14] to first estimate $\Delta_{\ell,u,v}$, and then localize the target.
- *ALRA:* Replace the channel estimation algorithm in *DFT* with the ALRA method [15].

The squared error (SE) of the position coordinate is used to evaluate the localization accuracy of each algorithm. Notice that BPSO, DFT, and ALRA all require random samples. We let $T = 3000$ by default.

We first sweep through different transmit power levels to examine different algorithms. Specifically, the transmit power varies from -10 dBm to 10 dBm in increments of 5 dBm. Fig. 8 shows the SNR boost achieved by different algorithms versus the transmit power. It can be seen that the SNR boost achieved by all algorithms increases with transmit power. Furthermore, it can also be seen that the proposed BPSO consistently achieves the highest SNR boost. Fig. 9 further shows the SE achieved by different algorithms versus the transmit power. Observe that higher transmission power consistently results in lower estimation errors for all algorithms. Observe also that the SE of *MUSIC-ZPS* is considerably higher than that of the system without MTSs due to the interference introduced by the two MTS in angle estimation. Observe also that the localization error by the proposed BPSO is less sensitive to the change of SNR.

We then vary the number of random samples T. In particular, we increase T from 1000 to 3000 in increments of 500, with the transmit power level fixed at $P = 0$ dBm. Fig. 10 shows the SNR boost achieved by different algorithms versus the number of samples T. As expected, the SNR boosts achieved by all algorithms increase with T, except for ZPS. Furthermore, the proposed BPSO algorithm consistently outperforms the CSI-based methods by more than 2 dB. Fig. 11 further shows the SE achieved by different algorithms versus the number of samples T. Observe that the two CSI-based methods perform even worse than the *MUSIC* method,

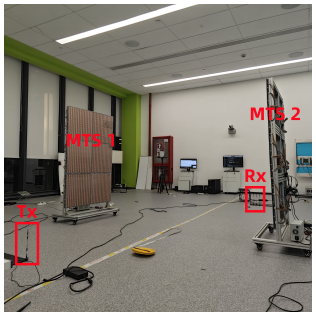

Fig. 6. Field Test Scenario.

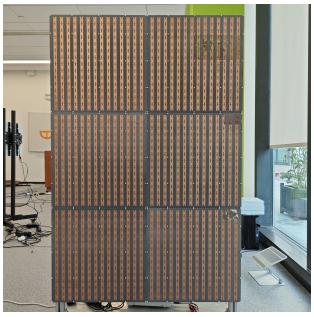

Fig. 7. MTS prototype.

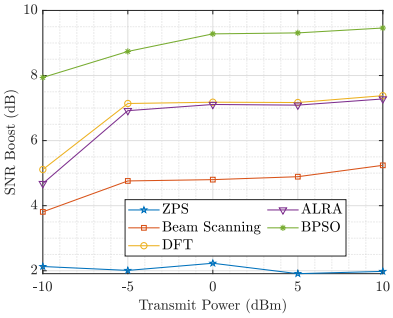

Fig. 8. SNR boost v.s. transmit power.

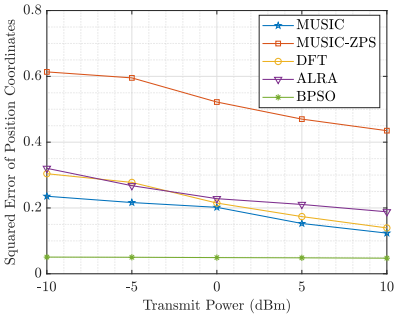

Fig. 9. Squared error v.s. transmit power.

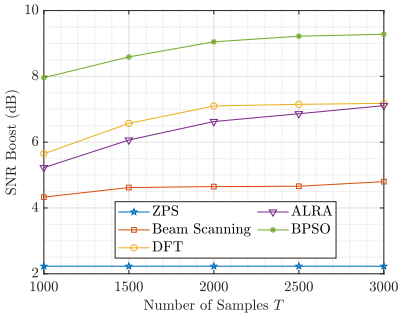

Fig. 10. SNR boost v.s. number of samples T.

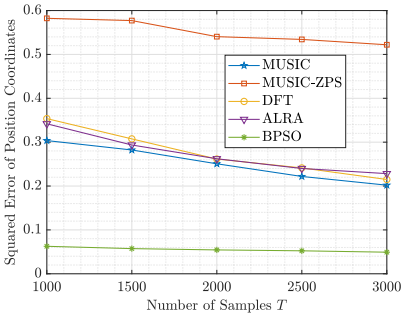

Fig. 11. Squared error v.s. number of samples T

indicating the poor performance of the channel estimation. In contrast, the proposed BPSO can achieve a notably low SE with only $T = 1000$ samples.

VII. Conclusion

This work proposes a blind beamforming approach to the joint enhancement of communication and localization. It hinges on two nontrivial observations. First, maximizing the conditional sample mean of RSS is equivalent to aligning reflected channels with the direct channel. Second, maximizing the conditional sample mean of RSS is also equivalent to the phase difference retrieval. Equipped with the above two equivalences, we propose an efficient algorithm that enables integrated communications and localization. Field test results show that the proposed algorithm outperforms benchmarks for both communication and localization tasks significantly.

References

[1] Q. Wu and R. Zhang, "Intelligent reflecting surface enhanced wireless network via joint active and passive beamforming," *IEEE Trans. Wireless Commun.*, vol. 18, no. 11, pp. 5394–5409, Nov. 2019.

[2] J. Yao, J. Xu, W. Xu, C. Yuen, and X. You, "Superimposed RIS-phase modulation for MIMO communications: A novel paradigm of information transfer," *IEEE Trans. Wireless Commun.*, vol. 23, no. 4, pp. 2978–2993, Apr. 2024.

[3] H. Shen, W. Xu, S. Gong, C. Zhao, and D. W. K. Ng, "Beamforming optimization for IRS-aided communications with transceiver hardware impairments," *IEEE Trans. Commun.*, vol. 69, no. 2, pp. 1214–1227, Feb. 2020.

[4] Z. Zhang, L. Dai, X. Chen, C. Liu, F. Yang, R. Schober, and H. V. Poor, "Active RIS vs. passive RIS: Which will prevail in 6G?" *IEEE Trans. Commun.*, vol. 71, no. 3, pp. 1707–1725, Mar. 2022.

[5] K. Feng, X. Li, Y. Han, S. Jin, and Y. Chen, "Physical layer security enhancement exploiting intelligent reflecting surface," *IEEE Commun. Lett.*, vol. 25, no. 3, pp. 734–738, Mar. 2020.

[6] V. Arun and H. Balakrishnan, "RFocus: beamforming using thousands of passive antennas," in *USENIX Symp. Netw. Sys. Design Implementation (NSDI)*, Feb. 2020, pp. 1047–1061.

[7] F. Gustafsson and F. Gunnarsson, "Mobile positioning using wireless networks: possibilities and fundamental limitations based on available wireless network measurements," *IEEE Signal Process. Mag.*, vol. 22, no. 4, pp. 41–53, Jul. 2005.

[8] H. Liu, H. Darabi, P. Banerjee, and J. Liu, "Survey of wireless indoor positioning techniques and systems," *IEEE Syst., Man, Cybern. Mag.*, vol. 37, no. 6, pp. 1067–1080, Nov. 2007.

[9] D. Xie, X. Wang, and A. Tang, "MetaSight: localizing blocked RFID objects by modulating NLOS signals via metasurfaces," in *Proc. Annu. Int. Conf. Mobile Syst., Appl., Service (MobiSys)*, 2022, p. 504–516.

[10] C. Li, Q. Huang, Y. Zhou, Y. Huang, Q. Hu, H. Chen, and Q. Zhang, "RIScan: RIS-aided multi-user indoor localization using COTS WiFi," in *Proc. ACM Conf. Embedded Netw. Sensor Syst. (SenSys)*, 2024, p. 445–458.

[11] K. W. Cho, M. H. Mazaheri, J. Gummeson, O. Abari, and K. Jamieson, "mmWall: A steerable, transflective metamaterial surface for nextG mmWave networks," in *USENIX Symp. Netw. Sys. Design Implementation (NSDI)*, 2023, pp. 1647–1665.

[12] L. Chen, B. Yu, J. Ren, J. Gummeson, and Y. Zhang, "Towards seamless wireless link connection," in *Proc. Annu. Int. Conf. Mobile Syst., Appl., Service (MobiSys)*, 2023, p. 137–149.

[13] S. Ren, K. Shen, Y. Zhang, X. Li, X. Chen, and Z.-Q. Luo, "Configuring intelligent reflecting surface with performance guarantees: Blind beamforming," *IEEE Trans. Wireless Commun.*, vol. 22, no. 5, pp. 3355–3370, May 2023.

[14] B. Zheng and R. Zhang, "Intelligent reflecting surface-enhanced OFDM: Channel estimation and reflection optimization," *IEEE Wireless Commun. Lett.*, vol. 9, no. 4, pp. 518–522, Apr. 2020.

[15] G. Yan, L. Zhu, and R. Zhang, "Power measurement enabled channel autocorrelation matrix estimation for IRS-assisted wireless communication," *IEEE Trans. Wireless Commun.*, vol. 24, no. 3, pp. 1832–1848, Mar. 2025.